Korean J. Chem. Eng., 35(3), 709-716 (2018)
DOI: 10.1007/s11814-017-0327-3

pISSN: 0256-1115
eISSN: 1975-7220

Removal of Acid Red G dye from aqueous solutions by adsorption to MCM-41-layered double hydroxides composite

Yisong Wang, Tao Du†, Lifeng Zhou, Yanli Song, Shuai Che, and Xin Fang

State Environmental Protection Key Laboratory of Eco-Industry, Northeastern University, Shenyang 110819, China
(*Received 4 September 2017 • accepted 22 November 2017*)

Abstract−MCM-41 supported layered double hydroxides (LDH) composite materials (ML) were synthesized and studied for removal of Acid Red G (ARG), an anionic dye, with the adsorption method. ML was prepared using in situ synthesis procedure for the low supersaturation coprecipitation method, and ML10 and ML20 presented promising application towards ARG dye adsorption capacity in industrial wastewater. Powder samples were characterized by X-ray diffraction, FTIR spectroscopy, scanning electron microscopy and energy dispersive spectrometry. The effects of different reaction time, initial solution pH and temperature on the dye adsorption capacity were investigated. Adsorption process was well described by pseudo-second-order kinetic model and Langmuir isotherm model. The fitting curves showed that ML10 and ML20 had higher adsorption rates and maintained a certain theoretical saturated adsorption capacity (92.19807 mg/g and 96.41947 mg/g, respectively) compared with LDH.

Keywords: Wastewater Treatment, Adsorption, Layered Double Hydroxides, MCM-41, Acid Red G

INTRODUCTION

With the rapid development of economic globalization, the treatment of wastewater has become a major environmental problem in textile, cosmetics, paper, leather, pharmaceutical, food, and other industries [1,2]. In them wastewater is an important source of water pollution, because it is resistant to degrading and threatens human health as an organic carcinogen [3,4]. Hence, there is a strong desire for research an effective method to remove dyes from effluents.

Some conventional commercial methods for removing dyes, such as coagulation, ultrafiltration, zonation, oxidation, sedimentation, reverse osmosis, flotation, precipitation and anaerobic microbial degradation, have certain defects and limitations in application, taking into account economy and practicability [5]. Although microbial technology is economically advantageous in commercial applications, its type of organic dye is limited [6]. Adsorption method to remove the dye in the waste water has the advantages of excellent removal efficiency, simple process and low equipment cost, and is widely regarded as one of the economic and promising methods for purifying and separating impurities in waste water [7]. Many conventional sorbents have been explored in the removal of dyes from wastewater, such as, resin [8,9], bentonite [10,11], zeolite [12], carbon nanotubes [13], coal based sorbents [14], coal fly ashes [15], and Mg-Al-layered double hydroxide [16]. However, the traditional adsorbents have been modified into composite adsorbents to remove dyes from wastewater that have been widely researched recently [17].

Layered double hydroxides (LDH) as a class of anionic clays have attracted considerable attention due to the intercalation assembly characteristic and functional applications. The chemical compositions of LDH materials are expressed by the general formula $[M_{(1-x)}^{2+}M_x^{3+}(OH)_2]A_{x/n}^{n-}\cdot mH_2O$, and its nanoscale two-dimensional laminates along the longitudinal arrangement into a three-dimensional crystal structure. In the above formula, A^{n-} are various interlayer inorganic anions or organic anions with negative charge n, x is the value of the $M^{3+}/(M^{2+}+M^{3+})$ ratio, and the synthesis of pure hydrotalcite needs x in a range of 0.1-0.33 [18], and m is the number of interlayer water molecules and equal to $(1-3x/2-\Delta)$ where Δ is below about 0.125 [19]. In recent years, LDH composite materials as adsorbent to remove the dye from aqueous solutions have become a research focus. Jiao et al. [20] successfully prepared the composites of magnetic iron oxide and LDHs (Fe/LDHs) that can effectively adsorb Acid Flavine 2G (AF 2G) from wastewater solution. Jia et al. [21] reported that MgAl-LDH/$CoFe_2O_4$ and MgAl-CLDH/$CoFe_2O_4$ nanofibers were prepared and investigated for the effective removal of Congo Red (CR) from aqueous solution. Zhang et al. [22] fabricated a composite via direct assembly of surface passivated carbon dots on the surface of the positively charged LDH, and found that it could be particularly efficient in removing Methyl Blue (MB). In 1992 Mobil Co. reported the synthesis of the ordered mesoporous silica molecular sieves of MCM-41 [23]. MCM-41 was considered suitable as a support material for composite adsorbents due to its high specific surface area, abundant pore structure, excellent thermal stability and physico-chemical stability. Bayramoglu et al. [24] constructed a novel MCM-41 silica particle grafted with polyacrylonitrile that has enhanced adsorption capacity for uranium ions from aqueous medium. Arica et al. [25] reported that magnetic MCM-41 composite particles were prepared and then grafted with poly(glycidyl methacrylate) for the adsorptive removal of Direct Blue 6 (DB-6) dye and Direct Black-38 (DB-38) dye from aqueous medium. The

†To whom correspondence should be addressed.
E-mail: dutao2000@hotmail.com

respective advantages of both materials can be fully exploited due to the combination of LDH and MCM-41. To our best knowledge, adsorption of Acid Red G (ARG) dye on LDH with MCM-41 composite materials adsorbent has not been investigated before.

In the present work, MCM-41 supported LDH composite materials (ML) were synthesized via in situ synthesis procedure for the low supersaturation coprecipitation method, and as adsorbent were examined for the removal of ARG dye from aqueous solutions. The structural and chemical properties of the synthesized LDH and ML were characterized by XRD, FTIR, SEM and EDS. The effects of different contact time, solution pH and reaction temperature on the adsorption performance of dyes in wastewater were investigated by the batch of comparing experiments. Experimental data were fitted with adsorption kinetics models, Freundlich and Langmuir models to research the interaction between adsorbents and dye.

MATERIAL AND METHODS

1. Materials

All the materials and reagents used in the synthesis process were analytical grade and all solutions were prepared with deionized water. Acid Red G ($C_{18}H_{13}N_3Na_2O_8S_2$, >99.5%) was purchased from TCI Development Co., Ltd. HCl, NaOH and Na_2CO_3 were obtained from Tianjin HengXing Chemical Reagent Co., Ltd. Others including $Mg(NO_3)_2{\cdot}6H_2O$, $Al(NO_3)_3{\cdot}9H_2O$, cetyl trimethyl ammonium bromide (CTAB), ethyl acrylate (EA) and tetraethoxysilane (TEOS) were obtained from Sinopharm Chemical Reagent Co., Ltd.

2. Synthesis of MCM-41

MCM-41 as a composite support material was synthesized following the hydrothermal method of Lin et al. [26]. CTAB, EA (70 wt%) and distilled water were combined at room temperature before TEOS was slowly added under vigorous stirring until the solution became homogeneous. The starting mixture with the composition $1.0SiO_2 : 0.15CTAB : 1.6EA : 120H_2O$ was stirred for 4 h and then transferred into a stainless steel autoclave with Teflon liner and heated at 373 K for 48 h. After the hydrothermal process, the product was filtered out, washed with distilled water until the pH reached 7 and dried at 363 K in the oven. The organic template in the sample was removed by calcining at 823 K for 6 h in a high temperature furnace, and the rate of heating was controlled at 1 K/min from room temperature and then dropped through air-cooling environment.

3. Synthesis of LDH

The Mg-Al type LDH was synthesized by low supersaturation coprecipitation method of Bhatta et al. [27]. Solution A containing 11.5 g of $Mg(NO_3)_2{\cdot}6H_2O$ and 8.4 g of $Al(NO_3)_3{\cdot}9H_2O$ was dissolved in 22.5 mL distilled water with a Mg/Al atomic ratio of 2 : 1. Solution B containing 4.24 g of Na_2CO_3 was dissolved in 15 mL distilled water. Solution C containing 6.4 g of NaOH and solution A were added dropwise simultaneously into solution B to maintain pH in the range of 10 to 12. The pH was monitored using a Model PHS-3C pH meter (Qiwei Instrument, China). The mixture was stirred for 24 hours at room temperature. The resulting precipitate was separated by centrifugation, washed with distilled water until the pH value was reduced to 7 and then 5.0 g of obtained sample was dried at 363 K in the oven.

4. Synthesis of ML

The in situ synthesis procedure for the low supersaturation coprecipitation method was described as follows: 1.25 g of MCM-41 was impregnated with the above solution B before it was added dropwise simultaneously with the above solution A and solution B maintaining a constant pH of 10-12. The mixture was stirred for 12 hours at 333 K. This composite material was separated by centrifugation, washed with distilled water until the pH value was reduced to 7 and dried at 363 K, and it was abbreviated as ML20. In addition, synthesis procedures of ML10, ML30, ML40 and ML50 were similar to the above ML20, where the numeral indicates the mass percentage of MCM-41 loading in the composites.

5. Characterization Methods

X-ray diffraction (XRD) patterns of LDH and ML were obtained by using an XRD-7000 diffractometer (Shimadzu, Japan) with Cu-Kα radiation that had the highest power of 40 kW. FTIR spectra of the samples were measured in the spectral range of 4,000-500 cm^{-1} on a Cary 660 Spectrum One FTIR spectrometer (Agilent Technologies, Australia). To analyze the surface morphology of materials, scanning electron microscope (SEM) images were obtained by using a EVO Element scanning electron microscope (ZEISS, Japan) using a beam voltage of 15 kV, which was coupled with an energy dispersive spectrometer (EDS) to identify the elemental composition content of samples.

6. Adsorption Experiments

All the adsorption experiments were performed in a series of flasks on a constant temperature magnetic stirrer. The suspension containing a certain concentration of Acid Red G and adsorbents (LDH or ML) was magnetically stirred for a certain time. Then the supernatant was achieved by centrifugation at 8,000 rpm for 3 min and analyzed by the UV-Vis spectrophotometer (Analytik Jena, Germany) to evaluate the adsorption capacity of all adsorbents. Adsorption capacity of adsorbent was measured by the differences between the initial and final dyes concentration in the equilibrium solution, and the absorbance values of ARG were recorded at the wavelength of 503 nm.

To study kinetic adsorption behavior, 50 ml concentration of 25 mg/g ARG solution and 50 mg of adsorbent were added into the flask in order and then magnetically stirred for 0 to 120 min at appropriate time intervals on 293 K. The effect of solution initial pH on adsorption capacities was surveyed by adjusting the desired pH of ARG solution with HCL or NaOH solution (1 mol/L) from 2 to 11. The effect of temperature on adsorption capacities experiment was determined at different temperatures (273, 293, 313, 333 and 353 K). For the adsorption isotherms experiment, ARG solution was prepared as a solution with a concentration from 50 to 400 mg/g at 50 mg/g concentration intervals for 60 min to achieve adsorption equilibration.

RESULTS AND DISCUSSION

1. Characterization

X-ray diffraction (XRD) patterns of the samples are shown in Fig. 1. These XRD patterns were compared with each other to confirm the structure of the samples and to determine whether

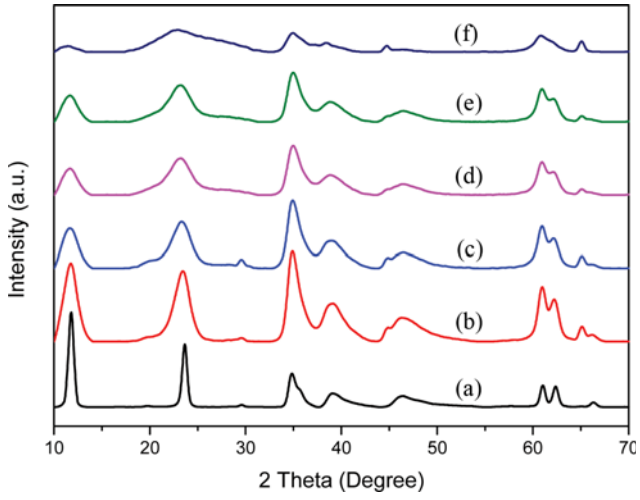

Fig. 1. XRD patterns of the samples. (a) LDH, (b) ML10, (c) ML20, (d) ML30, (e) ML40, and (f) ML50.

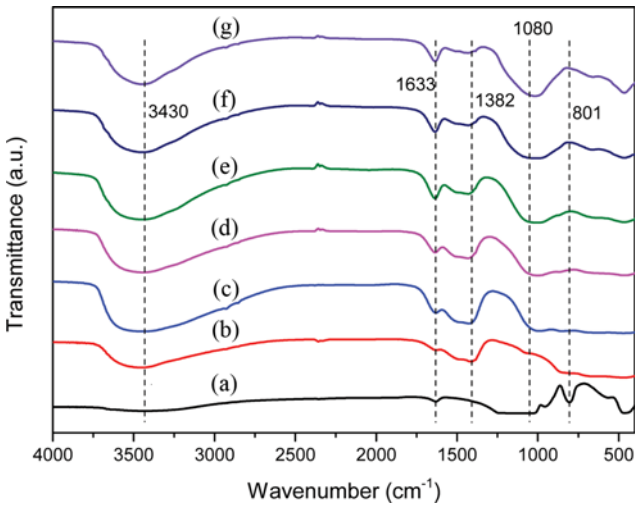

Fig. 2. FTIR spectra of the samples. (a) MCM-41, (b) LDH, (c) ML10, (d) ML20, (e) ML30, (f) ML40, and (g) ML50.

LDH was successfully combined with MCM-41. The presence of three intense reflection peaks close to ~11°, ~23° and ~35° (2θ) was ascribed to the diffractions by basal planes of (003), (006) and (009) reflections, and less intense characteristic pair of (110) and (113) reflection near 60° (2θ). This indicated that the synthesized samples were well crystallized, and the low angle reflection peak at 11.3° confirmed the presence of the intercalated carbonate ions in the LDH layer. These structural features were similar to the reported information in the literature [28-30]. There was an absence of crystalline by-products such as magnesium oxide or metal hydroxides, suggesting the purity of synthetic products. As the load content of MCM-41 increased, the reflection signal of the composites became weaker, which may be because the admixture was amorphous or the synthesis process affected the LDH crystal formation.

The FTIR spectra of LDH and ML are illustrated in Fig. 2. The spectrum of MCM-41 and ML shows bands at 1,080 cm^{-1} and 801 cm^{-1} which were due to asymmetric stretching of Si-O-Si and the corresponding symmetric stretching, respectively [31]. Absorption bands around 3,430 cm^{-1} for all samples are indicative of water and -OH stretching groups present on the surface or interlayer water molecules, and the band at 1,633 cm^{-1} was due to -OH bending vibration of water molecules [32]. The band of LDH and ML at 1382 cm^{-1} could be observed, which was attributed to the symmetry of carbonate anions being close to free anions [33]. These characteristic spectra again demonstrate that the layered structure of the combined LDH was complete as the loading of MCM-41 increased.

The scanning electron microscope images of MCM-41 and ML20 are presented in Fig. 3. We observed that the particle size of MCM-41 was relatively homogeneous and well dispersed with no obvious agglomeration. Therefore, it appeared that it could evenly load the LDH surface. Clearly, in Fig. 3(B), the MCM-41 particles were well supported on the surface of the platelet-shaped LDH. As shown in Fig. 4, the composition of the samples was quantitatively determined by EDS analysis. In contrast to the EDS spectrum data of pure LDH, characteristic peaks of the silicon element newly appeared due to the loading of MCM-41. The elemental

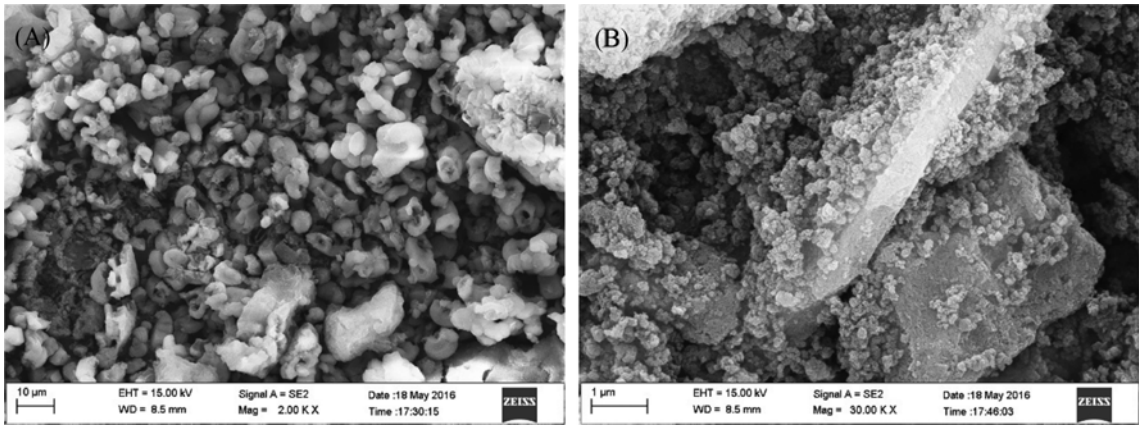

Fig. 3. SEM images of (A) MCM-41, and (B) ML20.

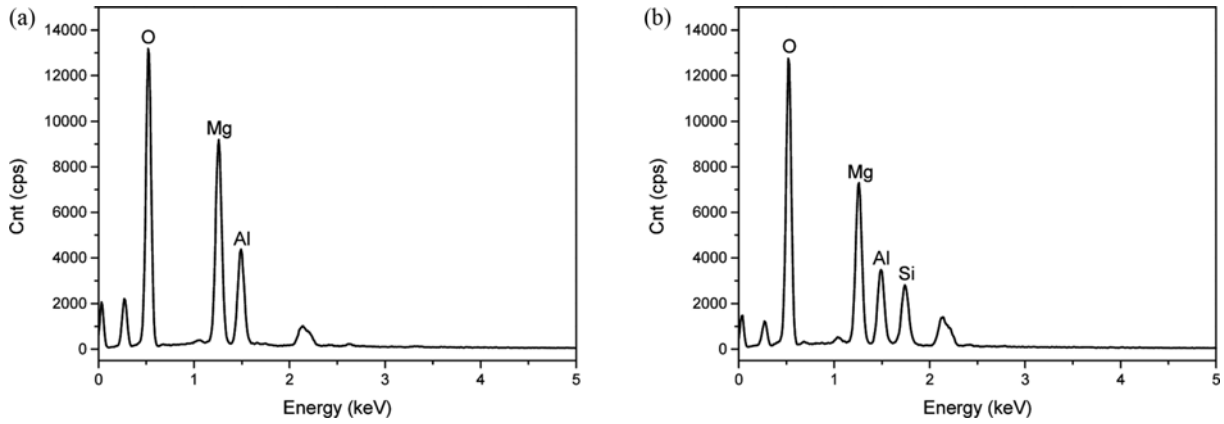

Fig. 4. EDS analysis of (a) LDH, and (b) ML20.

Table 1. Chemical composition of LDH and ML20 from EDS analysis

Sample	Chemical composition (wt%)				Mg/Al molar ratio	SiO_2/sample wt. ratio
	O	Mg	Al	Si		
LDH	54.42	28.18	17.41	0	1.80	0
ML20	54.67	22.08	12.71	10.54	1.93	0.2254

component content represented by the respective characteristic peaks of samples is summarized in Table 1. The molar ratio of Mg/Al in all samples was approximately 2 : 1, which was the same as the expected calculation at the time of synthesis. A similar analysis was reported in the literature [34]. The mass fraction of MCM-41 was calculated to be about 20 wt% of the composite by the ratio of the atomic mass of the Si and the other elements in the ML20, which was also in line with the expected loading.

2. Adsorption Kinetics

The adsorption mechanism and adsorption characteristics of adsorbent adsorbed dye ARG were studied by adsorption kinetics experiment and kinetics model. The adsorption kinetics experiment of ARG on LDH and ML powder was operated in regular time interval at room temperature. The data obtained from adsorption experiment were fitted by various kinetic models including the pseudo-first-order kinetics model (1) and pseudo-second-order kinetics model (2).

$$\lg(q_e - q_t) = \lg q_e - \frac{k_1}{2.303}t \quad (1)$$

$$\frac{t}{q_t} = \frac{1}{k_2 q_e^2} + \frac{1}{q_e}t \quad (2)$$

where q_e and q_t are the amounts of dyes (mg/g) adsorbed on the adsorbents at equilibrium and any time t, respectively; k_1 and k_2 are constants of pseudo-first-order and pseudo-second-order kinetic model for adsorption, respectively.

As shown in Fig. 5, adsorption quantity changes in LDH and ML with time were described experimental measurement points and the pseudo-second-order kinetic model [35] predictive curves. It is obvious that the LDH loaded with MCM-41, in comparison

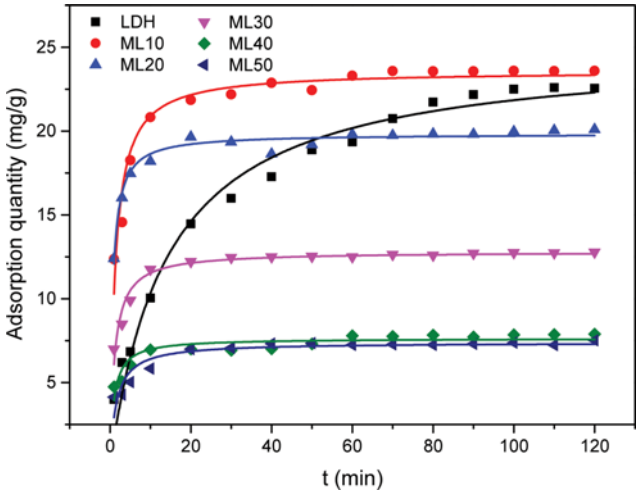

Fig. 5. The adsorption amount of ARG over samples as a function of time.

with the raw LDH, increased the adsorption rate and shortened the equilibrium time. However, with the increase of MCM-41 load ratio, the adsorption effect increased first and then decreased. Among them, quantity capacity of LDH, ML10 and ML20 was approximately the same, but the adsorption rate of ML10 was the largest within 120 minutes. Although the adsorption capacity of ML30, ML40, ML50 was clearly reduced owing to the increase of MCM-41 load ratio, especially the adsorption effect of ML40 and ML50 has been severely affected, their adsorption rate was still increased at the initial time. The calculated parameters of the pseudo-first-order kinetic [36] and pseudo-second-order kinetic models for adsorption of LDH and ML are shown in Table 2. Compared with the pseudo-first-order kinetic model?the values of the correlation coefficients of the pseudo-second-order kinetic model are more perfect (Maximum R^2=0.9756), indicating the adsorption behaviors of the five adsorbents in the whole range of considered time can be described. Meanwhile, it is suggested that LDH and ML were chemically adsorbed on ARG and chemisorption usually is considered irreversible. The result of the model was built on the adsorption quantity of dye adsorbed, and it will help to predict the adsorption behavior over the entire concentration

Table 2. The calculated parameters of the pseudo-first-order and pseudo-second-order kinetic models for adsorption of LDH and ML

Kinetic model	Parameters	LDH	ML10	ML20	ML30	ML40	ML50
Pseudo-first-order	q_e (mg/g)	22.8569	21.5774	19.3174	12.4247	7.3995	7.1435
	k_1 (1/min)	0.4250	0.0547	0.8625	0.4808	0.5912	0.3436
	R^2	0.7858	0.9400	0.7906	0.7841	0.5432	0.6389
Pseudo-second-order	q_e (mg/g)	23.5887	24.9328	19.8383	12.8005	7.6355	7.3881
	k_2 (g/(mg min))	0.0329	0.0028	0.0784	0.0708	0.0271	0.0883
	R^2	0.9416	0.9756	0.9660	0.9502	0.8207	0.8485

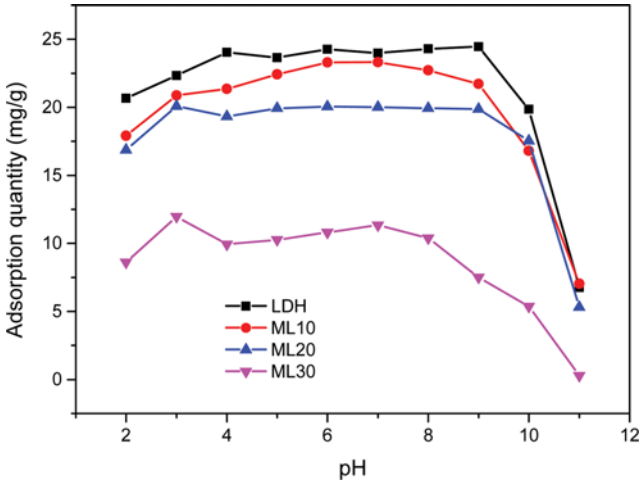

Fig. 6. Effect of initial solution pH on adsorption quantity of dye by LDH and ML.

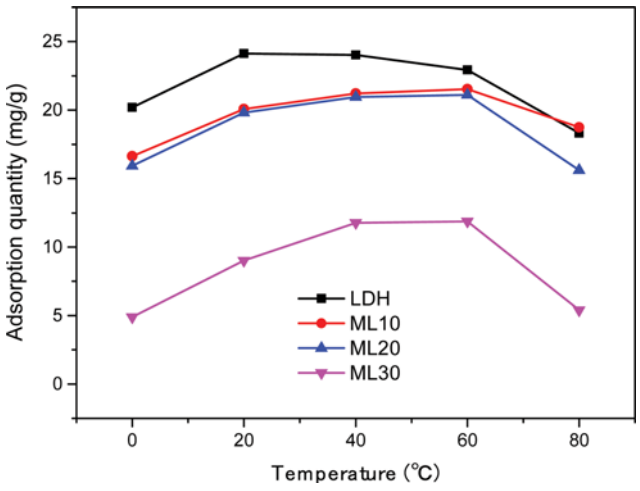

Fig. 7. Effect of solution temperature on adsorption quantity of dye by LDH and ML.

range and time range, and as a rate control mechanism to support chemical adsorption [37]. Furthermore, the mechanism of adsorption, in addition to the physical and chemical properties of the adsorbent, was also determined by the mass transfer process [38]. The ML, which was compounded by mesoporous materials, thus increased the mass transfer rate, and then its adsorption rate increased, showed a greater advantage for dye adsorption.

3. Effect of Initial pH on Adsorption

The data on the effect of the initial solution pH on the dye adsorption capacity were recorded in Fig. 6, where LDH and ML were used as adsorbents, and experiments were performed under various initial solution pH values ranging from 2 to 11 under the same operating conditions. It is clearly shown that the adsorption quantity of the adsorbents was relatively stable at the initial solution pH of 2 to 9, and then significantly reduced with further increasing pH value. Several aspects, such as adsorption capacity of adsorbent, surface charges and active sites, may be attributed to the adsorption behavior of the adsorbent under different solution pH values [39]. Compared with pure LDH, the complex ML had a similar trend to the adsorption capacity at different pH values, since the surface with CO_3-LDH contained a large number of chemically active sites. The point of zero charge (PZC) is a qualitative analysis of the adsorbent surface charge balance parameters, and can be used to explain the effect of solution pH on adsorption capacity [40]. According to the PZC theory, when pH<PZC, the adsorbent surface is positively charged, which enhances the adsorption capacity of negatively charged anionic dyes by electrostatic attraction force. ARG is a type of anionic dye, so the electrostatic attraction force contributed to the adsorption behavior in this pH range between 2 and 9. The composite ML had no change in the characteristics and mechanism of the effect of acidity on the adsorption properties of the solution, and still had a wide range of pH adsorption applications that are similar to LDH.

4. Effect of Temperature on Adsorption

Effect of dye solution temperature on the adsorption capacity of LDH and ML at 0-80 °C is presented in Fig. 7. It is obvious that the adsorption capacity of LDH and ML to dyes was relatively stable in the range of 20 to 40 °C, and out of this range they had a decrease in adsorption capacity at lower temperatures of 0 °C and higher temperatures of 80 °C. At lower temperatures, the Brownian motion of dye molecules is weak, which reduces the contact of dye molecules with the adsorbents, leading to less adsorption [41]. On the other hand, the decreased trend of ML adsorption quantity was more pronounced at higher temperature of 80 °C, may be due to the collapse of the hydrogen bond or physisorption of dye on MCM-41 surface. The experiment was carried out in a constant temperature oil bath in the laboratory. ML was not significantly reduced in temperature range owing to the complex, and it can still be adapted to the relatively wide temperature requirements of industrial dye wastewater.

5. Adsorption Isotherms

To identify a suitable model for design purposes, the adsorp-

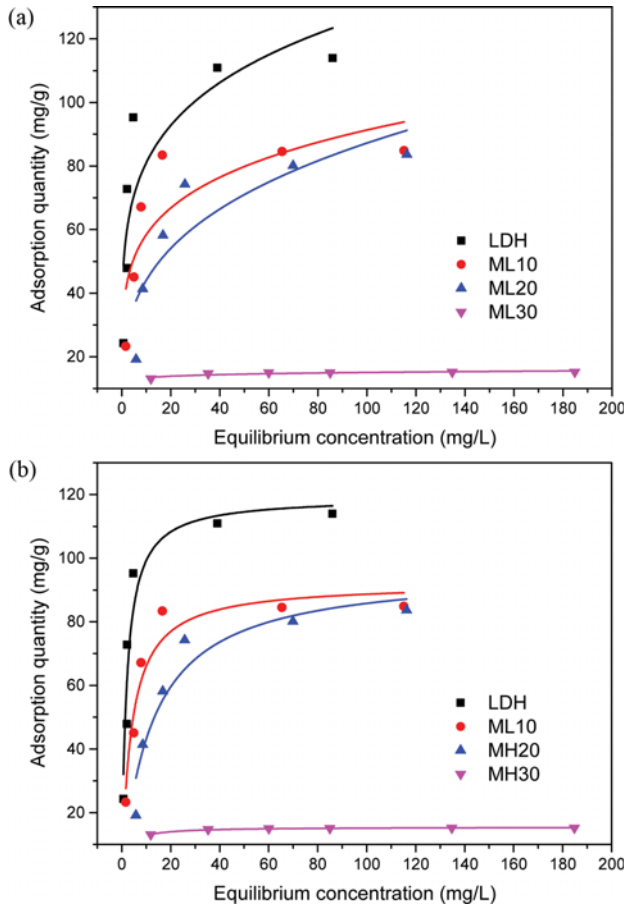

Fig. 8. Adsorption isotherms of ARG dye on LDH and ML. (a) Freundlich isotherm, (b) Langmuir isotherm.

tion isotherms were carried out to estimate the adsorption characteristics between dye and adsorbent. The equilibrium adsorption experimental data obtained in this study were analyzed by the commonly used Freundlich and Langmuir isotherm models. The experimental data and the results of the two fitting models are shown in the Fig. 8. The Freundlich adsorption isotherm is a widely applicable equation for many adsorption solutions, which is assumed that adsorption occurs on non-uniform surfaces. The Freundlich isotherm model is expressed by the following equation [42]:

$$\lg q_e = \frac{1}{n}\lg c_e + \lg k \quad (3)$$

where q_e (mg/g) and c_e (mg/L) are the equilibrium adsorption quantity of adsorbents and equilibrium adsorbate concentration of solution, k and 1/n are Freundlich isotherm constants which are as indicative of the extent of adsorption and adsorption intensity.

Langmuir theory suggests that the adsorption sites can be evenly distributed over the entire interaction surface, but more non-uniform distribution. Langmuir isotherm model can be described by the following equation [43]:

$$\frac{c_e}{q_e} = \frac{1}{bq_m} + \frac{c_e}{q_m} \quad (4)$$

where q_e (mg/g) and c_e (mg/L) are the equilibrium adsorption quantity of adsorbents and equilibrium adsorbate concentration of solution, q_m (mg/g) is the maximum sorption capacity, and b (L/mg) is the Langmuir constant related to the free energy of adsorption.

The parameter values such as k, 1/n, q_m, b and the correlation coefficients for Freundlich and Langmuir models obtained by non-linear curve fitting are listed in Table 3. It is clearly shown that the value of correlation coefficients (R^2=0.90791, 0.92512, 0.90276, 0.99061) for the Langmuir model was much closer to 1 than that of Freundlich model. Therefore, the adsorption isotherm of ARG dye on LDH and ML was more suitably described by Langmuir isotherm model, compared with Freundlich isotherm model. On the other hand, both LDH and ML were on a higher level of fit-

Table 3. Adsorption isotherm parameters of ARG dye on LDH and ML

Model	Parameters	LDH	ML10	ML20	ML30
Freundlich model	k	51.63467	37.31673	22.23065	11.93036
	1/n	0.19558	0.19434	0.29681	0.05044
	R^2	0.68403	0.64201	0.72518	0.78597
Langmuir model	q_m (mg/g)	119.17696	92.19807	96.41947	15.44052
	b (L/mg)	0.49647	0.25202	0.08074	0.48074
	R^2	0.90791	0.92512	0.90276	0.99061

Table 4. Comparison of adsorbents for dye removal from the literature and the present study

Adsorbents	Dye used	Adsorption capacity (mg/g)	References
Fe/CLDH	Acid Flavine 2G	147	[20]
MgAl-LDH/$CoFe_2O_4$	Congo Red	213	[21]
LDH-carbon dot	Methyl Blue	185	[22]
p(GMA-EGMA)-TAA resin	Reactive Brown 10	162	[25]
Mg-Al-LDHs	Acid Red G	93	[28]
ML10	Acid Red G	92	This work
ML20	Acid Red G	96	This work

ting degree of Langmuir models, so they had the same adsorption characteristics. Theoretical adsorption capacity of ML10 (q_m= 92.19807 mg/g) and ML20 (q_m=96.41947 mg/g) was slightly lower than that of LDH, but still maintained a high value. However, according to the above description, the adsorbent adsorption rate of the composite was improved considerably. Comparison of adsorbents for dye removal from the literature and this work is summarized in Table 4. The adsorption capacity of ML10 and ML20 to remove ARG has a higher level in the present study. Therefore, ML10 and ML20 have a wide application prospect in adsorbing ARG dye wastewater.

CONCLUSIONS

A series of experimental results in this study showed that ML20 had higher adsorption rate and maintained a certain adsorption capacity compared with LDH for the removal of ARG dye from aqueous solution. XRD patterns, FTIR spectra, SEM images and EDS analysis of LDH and ML clearly show that MCM-41 particles were well supported on the surface of the platelet-shaped LDH, and the layered structure of the combined LDH was complete as the loading of MCM-41. The adsorption kinetics experimental data were analyzed and studied for the adsorption rate, which was consistent with the pseudo-second-order kinetic model. And the adsorption rate of ML was greater than LDH due to the loading of the mesoporous material to enhance the mass transfer rate. The adsorption performance of ML was excellent at a pH of 2 to 9 and had a wide range of pH adsorption applications. The adsorption capacity of LDH and ML to dyes was relatively stable in the range of 20 to 40 °C. Adsorption isotherm of ARG dye on LDH and ML was more suitably described by Langmuir isotherm model, and both had the same adsorption characteristics. The theoretical saturated adsorption capacity by ML10 and ML20 was 92.19807 mg/g and 96.41947 mg/g, respectively, indicating that ML10 and ML20 are more superior materials for application in the adsorption of ARG dye wastewater.

ACKNOWLEDGEMENTS

This work was funded by the National Natural Science Foundation of China (Grant No. 51474067). We also appreciate the efforts of anonymous reviewers of the Journal of Cleaner Production.

REFERENCES

1. B. Bi, L. Xu, B. Xu and X. Liu, *Appl. Clay Sci.*, **54**, 242 (2011).
2. L. El Gaini, M. Lakraimi, E. Sebbar, A. Meghea and M. Bakasse, *J. Hazard. Mater.*, **161**, 627 (2009).
3. A. K. Mittal and S. K. Gupta, *Water Sci. Technol.*, **34**, 81 (1996).
4. R. M. M. dos Santos, R. G. L. Gonçalves, V. R. L. Constantino, L. M. da Costa, L. H. M. da Silva, J. Tronto and F. G. Pinto, *Appl. Clay Sci.*, **80**, 189 (2013).
5. D. Chebli, A. Bouguettoucha, A. Reffas, C. Tiar, M. Boutahala, H. Gulyas and A. Amrane, *Desalination Water Treat.*, **57**, 22061 (2016).
6. V. M. Correia, T. Stephenson and S. J. Judd, *Environ. Technol.*, **15**, 917 (1994).
7. R. Shan, L. Yan, Y. Yang, K. Yang, S. Yu, H. Yu, B. Zhu and B. Du, *J. Ind. Eng. Chem.*, **21**, 561 (2015).
8. M. A. Kamboh, I. B. Solangi, S. T. H. Sherazi and S. Memon, *J. Hazard. Mater.*, **186**, 651 (2011).
9. F. Bildik, G. T. Turan, G. Barim and B. F. Senkal, *Sep. Sci. Technol.*, **49**, 1700 (2014).
10. N. Jovic-Jovicic, A. Milutinovic-Nikolic, I. Grzetic and D. Jovanovic, *Chem. Eng. Technol.*, **31**, 567 (2008).
11. D. Bombos, R. Ganea, V. Matei, C. Marinescu, A. Bodnarev, S. Mihai, T. Natu and I. Tamas, *Rev. Chim.*, **65**, 976 (2014).
12. M. Qiu, C. Qian, J. Xu, J. Wu and G. Wang, *Desalination*, **243**, 286 (2009).
13. M. H. Beyki, H. Alijani and M. H. Ghasemi, *Desalination Water Treat.*, **57**, 20565 (2016).
14. S. V. Mohan, N. C. Rao and J. Karthikeyan, *J. Hazard. Mater.*, **90**, 189 (2002).
15. P. Janos, H. Buchtova and M. Ryznarova, *Water Res.*, **37**, 4938 (2003).
16. R. Lafi, K. Charradi, M. A. Djebbi, A. Ben Haj Amara and A. Hafiane, *Adv. Powder Technol.*, **27**, 232 (2016).
17. G. Bayramoglu, A. Akbulut, G. Liman and M. Y. Arica, *Chem. Eng. Res. Des.*, **124**, 85 (2017).
18. K. Parida and J. Das, *J. Mol. Catal. Chem.*, **151**, 185 (2000).
19. H. F. W. Taylor, *Mineral. Mag.*, **39** (1973).
20. F. Jiao, J. Yu, H. Song, X. Jiang, H. Yang, S. Shi, X. Chen and W. Yang, *Appl. Clay Sci.*, **101**, 30 (2014).
21. Z. Jia, S. Li, J. Liu, Q. Qin and R. Zhu, *Bull. Mater. Sci.*, **38**, 1757 (2015).
22. M. Zhang, Q. Yao, C. Lu, Z. Li and W. Wang, *ACS Appl. Mater. Interfaces*, **6**, 20225 (2014).
23. C. T. Kresge, M. E. Leonowicz, W. J. Roth, J. C. Vartuli and J. S. Beck, *Nature*, **359**, 710 (1992).
24. G. Bayramoglu and M. Y. Arica, *Micropor. Mesopor. Mater.*, **226**, 117 (2016).
25. T. A. Arica, E. Ayas and M. Y. Arica, *Micropor. Mesopor. Mater.*, **243**, 164 (2017).
26. W. Lin, Q. Cai, W. Pang, Y. Yue and B. Zou, *Micropor. Mesopor. Mater.*, **33**, 187 (1999).
27. L. K. G. Bhatta, S. Subramanyam, M. D. Chengala, U. M. Bhatta and K. Venkatesh, *Ind. Eng. Chem. Res.*, **54**, 10876 (2015).
28. D. S. Tong, M. Liu, L. Li, C. X. Lin, W. H. Yu, Z. P. Xu and C. H. Zhou, *Appl. Clay Sci.*, **70**, 1 (2012).
29. G. Darmograi, B. Prelot, G. Layrac, D. Tichit, G. Martin-Gassin, F. Salles and J. Zajac, *J. Phys. Chem. C*, **119**, 23388 (2015).
30. S. Wang, Z. Li and C. Lu, *J. Colloid Interface Sci.*, **458**, 315 (2015).
31. A. K. Kushwaha, N. Gupta and M. C. Chattopadhyaya, *Desalination Water Treat.*, **52**, 4527 (2014).
32. R. Extremera, I. Pavlovic, M. R. Pérez and C. Barriga, *Chem. Eng., J.* **213**, 392 (2012).
33. W. H. Zhang, X. D. Guo, J. He and Z. Y. Qian, *J. Eur. Ceram. Soc.*, **28**, 1623 (2008).
34. J. M. Lee, Y. J. Min, K. B. Lee, S. G. Jeon, J. G. Na and H. J. Ryu, *Langmuir*, **26**, 18788 (2010).
35. Y.-S. Ho, *J. Hazard. Mater.*, **136**, 681 (2006).
36. A. Özcan, E. M. Öncü and A. S. Özcan, *Colloids Surf. Physicochem. Eng. Asp.*, **277**, 90 (2006).

37. N. Buvaneswari and C. Kannan, *J. Hazard. Mater.*, **189**, 294 (2011).
38. T. Xue, Y. Gao, Z. Zhang, A. Umar, X. Yan, X. Zhang, Z. Guo and Q. Wang, *J. Alloys Compd.*, **587**, 99 (2014).
39. I. M. Ahmed and M. S. Gasser, *Appl. Surf. Sci.*, **259**, 650 (2012).
40. F. P. de Sá, B. N. Cunha and L. M. Nunes, *Chem. Eng. J.*, **215**, 122 (2013).
41. J. Liu, X. Li, J. Luo, C. Duan, H. Hu and G. Qian, *Chem. Eng. J.*, **242**, 187 (2014).
42. H. M. F. Freundlich, *Z. Phys. Chem. Leipz.*, **57A**, 385 (1906).
43. I. Langmuir, *J. Am. Chem. Soc.*, **38**, 2221 (1916).